Magnetic properties of $La_{0.67}Sr_{0.33}MnO_3/YBa_2Cu_3O_7$ superlattices

P. Przyslupski, I. Komissarov, W. Paszkowicz, P. Dluzewski, R. Minikayev, and M. Sawicki
Institute of Physics, Polish Academy of Sciences, 02–668 Warszawa, Poland
(Received 8 October 2003; published 29 April 2004)

Oxide multilayers composed of ferromagnetic metallic layers of $La_{0.67}Sr_{0.33}MnO_3$ (LSMO) and superconducting cuprate $YBa_2Cu_3O_7$ (YBCO) were grown on (1 0 0) $LaAlO_3$ substrates by high-pressure dc sputtering. We have investigated structural, transport, and magnetic properties of a series of samples in which the layer thickness of LSMO is fixed at 16 unit cells and that of YBCO varied from 1 to 8 unit cells. Exchange-induced unidirectional anisotropy in LSMO/YBCO superlattices has been demonstrated. Observation of an exchange biasing effect in LSMO/YBCO superlattices supports an existence of interlayer exchange coupling between LSMO layers through YBCO superconducting spacer layers.

DOI: 10.1103/PhysRevB.69.134428 PACS number(s): 74.78.Fk, 75.60.−d, 75.70.Cn

I. INTRODUCTION

Superconducting (S) and ferromagnetic (F) multilayers are interesting from fundamental point of view, since they offer the appropriate scenario to study competing effects of superconductivity and ferromagnetism on the scale of their characteristics lengths. The proximity effect in S/F multilayers is related to new physical phenomena arising from the interaction between two order parameters. For example, it was theoretically predicted[1,2] that a magnetic interlayer exchange coupling between ferromagnetic layers separated by *d*-wave superconductor is possible. The model suggests that the ground state of the S/F heterostructures changes from aligned magnetization to antiparallel magnetization with the period of two unit cells of the *c*-axis parameter of $YBa_2Cu_3O_7$ (YBCO) system. The interplay between superconductivity and spin-polarized systems has also potential applications in the emerging field of spin electronics.[3] The half metals are suitable materials in this respect. Half metallic behavior has been found experimentally in the manganese perovskite $La_{0.67}Sr_{033}MnO_3$ (LSMO).[4] The perovskites are particularly interesting because of their ability to form high-quality multilayers[5–9] with high-T_c superconductors (HTSC). Understanding the interface properties of colossal magnetoresistance materials (CMR) and HTSC heterostructures is required for spin-based devices. The key factor in such studies is electronic and magnetic quality of the interface region. Recent elipsometric measurements[10] of far infrared dielectric measurements provide an evidence of hole charge transfer from YBCO layers to LCMO layers in YBCO/LCMO superlattices. Due to this effect a dramatic depletion of holes for about 1 nm thick YBCO layer was observed. On the other hand an increase of holes in LCMO system in spite of nominal composition $La_{0.67}Ca_{0.33}MnO_3$ can drive the LCMO manganite into antiferromagnetic (AF) state. In this work we report and analyze some observations of structural and magnetic properties of LSMO/YBCO superlattices. If an effect of hole charge transfer takes place also in LSMO/YBCO superlattices it could transform some of the LSMO layers into F/AF system. It is known that when F/AF interfaces are cooled through the Neel temperature T_N an unidirectional anisotropy[11] (exchange biasing) may develop in LSMO layers. Exchange biasing is manifested as a displacement of the hysteresis loop along its field axis. Observation of the exchange biasing with superconducting spacer layers can indicate a presence of interlayer exchange coupling between LSMO layers through superconducting YBCO spacer layers.

II. EXPERIMENT

LSMO and YBCO thin films and LSMO/YBCO superlattices were deposited on (100) $LaAlO_3$ single-crystal substrates by multitarget high pressure sputtering.[6] During the growth, the temperature of the substrate was set at 770 °C and the oxygen pressure was kept at 3 mbar. Two targets with nominal composition of $La_{0.67}Sr_{0.33}MnO_3$ and $YBa_2Cu_3O_7$ were used for deposition. The thickness of different layers was controlled by the deposition times of respective targets. The calibrated deposition rates were 1.6 nm and 2.6 nm per minute for LSMO and YBCO, respectively. The off-axis x-ray diffraction measurements (Cu $K\alpha$ radiation) were used for structure characterization. The dc magnetization were measured with superconducting quantum interference device (SQUID) magnetometer in the temperature range 5 K–300 K in magnetic field up to 0.1 T. Microstructure properties of samples were examined by transmission electron microscope (TEM) JEOL 2000 EX. Samples used for SQUID measurements were 3 mm×3 mm in size. Resistance versus temperature measurements were performed with four-probe method.

TABLE I. Nominal modulation length, zero resistance temperature T_{c0}, and the temperature of the onset of diamagnetic moment T_{d0} of the $La_{0.67}Sr_{0.33}MnO_3$/YBCO multilayers.

Sample No.	Modulation length	T_{c0} [K]	T_{d0} [K]
LaY110	$[LSMO\times 16$ u.c./$YBCO\times 1$ u.c.$]_{16}$		
LaY105	$[LSMO\times 16$ u.c./$YBCO\times 2$ u.c.$]_{16}$	<4.2	
LaY107	$[LSMO\times 16$ u.c./$YBCO\times 3$ u.c.$]_{16}$	28	13
LaY109	$[LSMO\times 16$ u.c./$YBCO\times 4$ u.c.$]_{16}$	41	41
LaY106	$[LSMO\times 16$ u.c./$YBCO\times 5$ u.c.$]_{16}$	57	57
LaY108	$[LSMO\times 16$ u.c./$YBCO\times 6$ u.c.$]_{16}$	63	63
LaY111	$[LSMO\times 16$ u.c./$YBCO\times 8$ u.c.$]_{16}$	71	71

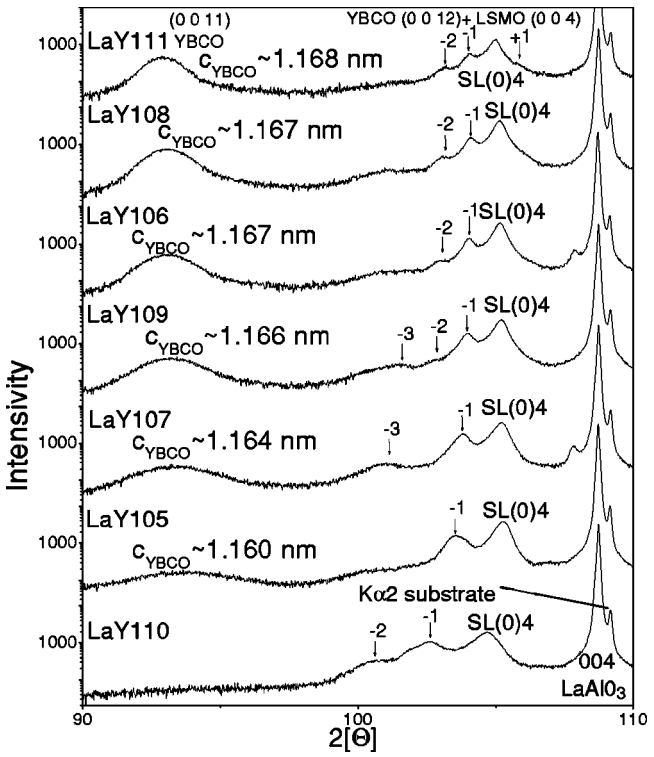

FIG. 1. High-angle x-ray diffraction pattern of LSMO/YBCO superlattices (Table I). Arrows represent the position of satellite peaks.

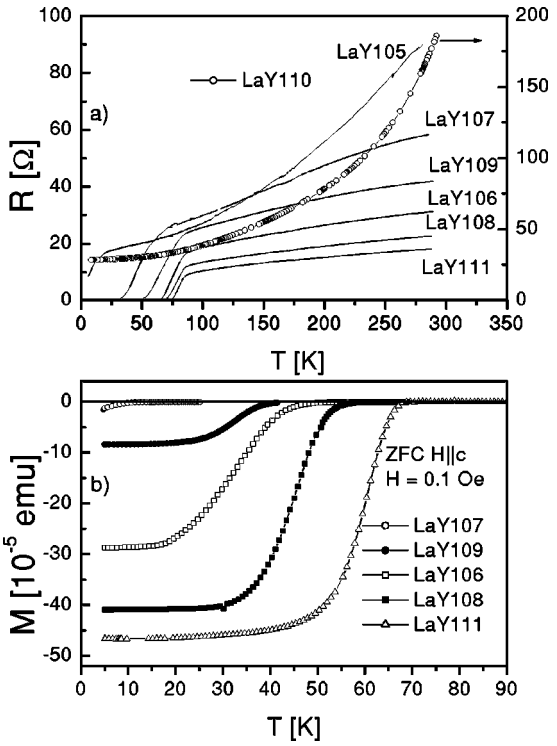

FIG. 3. (a) Resistance vs temperature of LSMO/YBCO superlattices (b) ZFC magnetic moment vs temperature for LSMO/YBCO superlattices.

III. RESULTS AND DISCUSSION

We have deposited $[\text{LSMO}\times 16\text{ u.c./YBCO}\times m\text{ u.c.}]_{16}$ multilayers (Table I) in which the LSMO layer thickness was fixed at $n=16$ unit cells (u.c.) while the YBCO layer thickness was varied from 1 unit cell to 8 unit cells. The *c*-axis lattice parameter for relaxed YBCO film is $c=1.168$ nm ($a=0.382$ nm and $b=0.388$ nm). The LSMO 100 nm thick film deposited on $LaAlO_3$ substrate has $a_\perp$ lattice parameter in a pseudocubic setting of about 0.396 nm, whereas for the bulk polycrystalline $La_{0.67}Sr_{0.33}MnO_3$ sample *a* is 0.387 nm. The spectra obtained from high-resolution x-ray diffraction studies of samples listed in Table I are plotted in the high-angle region (Fig. 1). In the high-angle spectrum a well-defined (0 0 11) YBCO Bragg peak of increasing intensity and superlattice peak SL(0)4 [(0 0 12) YBCO plus (0 0 4) LSMO] together with well resolved satellites of up to third order are found.

The estimated *c*-axis lattice parameter from the position

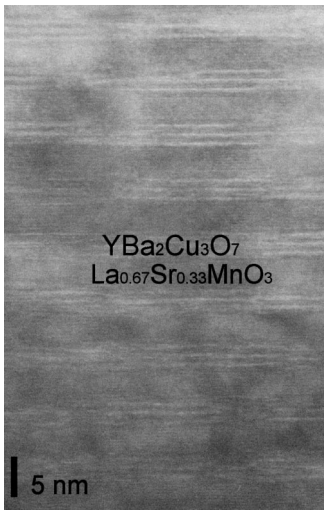

FIG. 2. TEM cross-section image of the $[\text{LSMO}\times 8\text{ u.c./YBCO}\times 3\text{ u.c.}]_{16}$ superlattice.

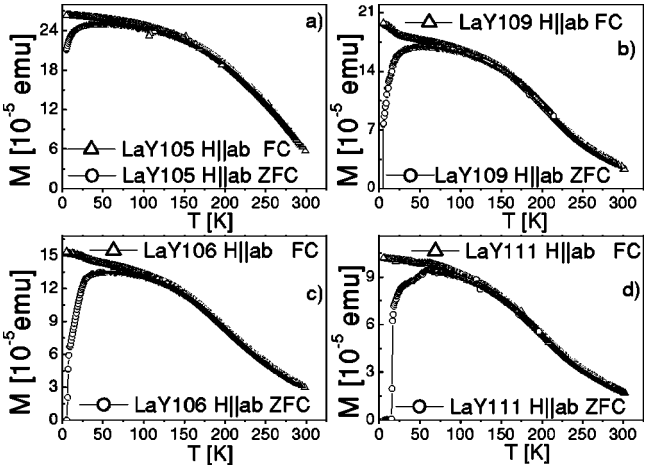

FIG. 4. ZFC and FC magnetic moment vs temperature in magnetic field of 500 Oe, for magnetic field parallel to the samples, $H\|ab$, superlattices with 2, 4, 5, and 8 unit cells YBCO layer thickness.

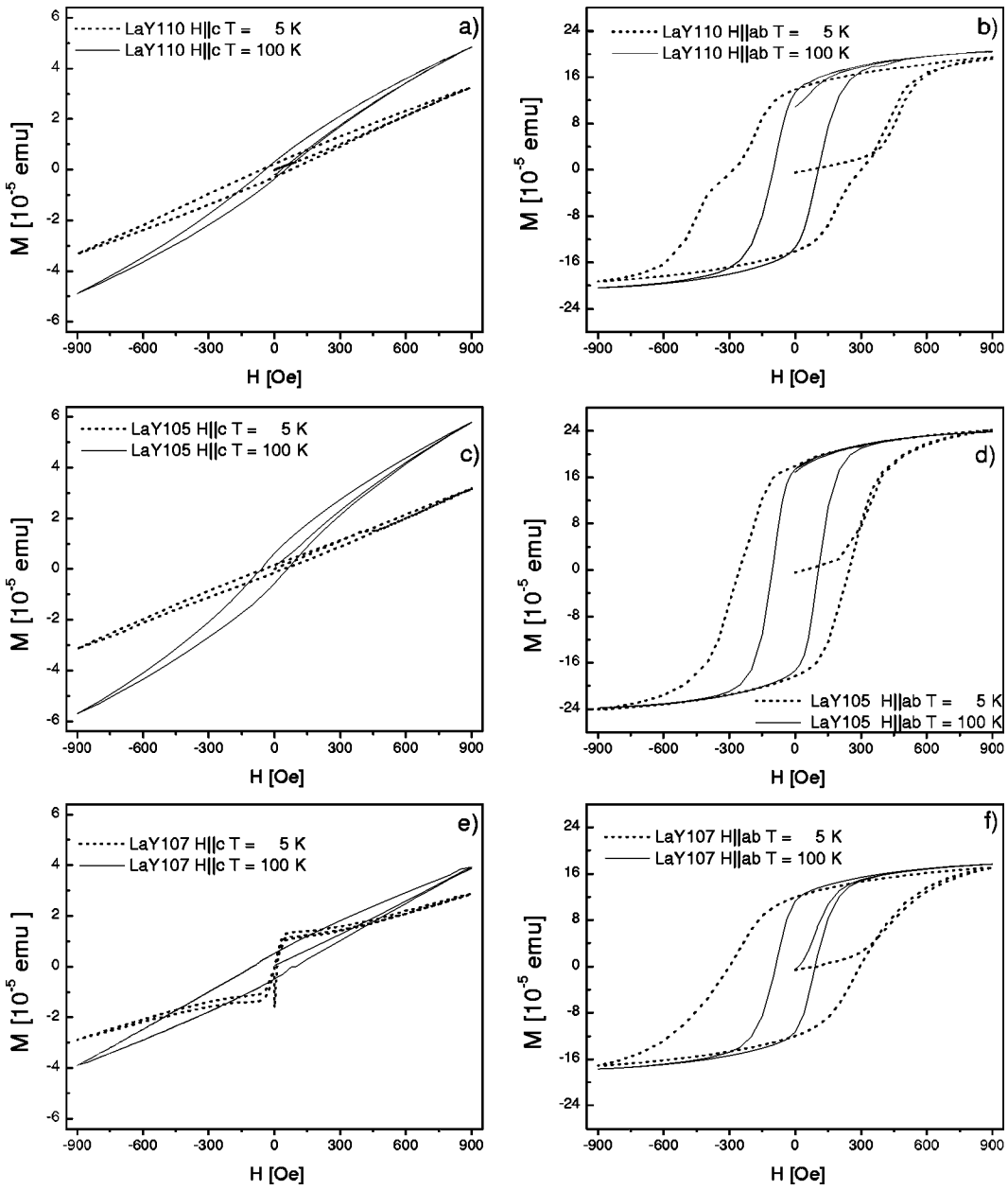

FIG. 5. Magnetization loops of the $[\mathrm{LSMO}\times 16\ \mathrm{u.c./YBCO}\times n\ \mathrm{u.c.}]_{16}$ for $n=1,2,3$ unit cells YBCO layer thickness superlattices measured at 5 K to 100 K temperature interval for magnetic field perpendicular ($H\|c$) and parallel ($H\|ab$) to the substrates.

of (0 0 11) Bragg peak for multilayer with 2 unit cells YBCO layer thickness is depressed ($c\sim 1.160$ nm).

The estimated *c*-axis lattice parameter for multilayer with 8 unit cells YBCO layer thickness is $c\sim 1.168$ nm, i.e., the same as for the relaxed YBCO film. This behavior demonstrates uniaxial compressive strain of YBCO layers along the [0 0 1] direction.

From the position of satellite peaks the modulation wavelength of the superlattices was estimated. Experimental modulation wavelengths are in agreement within 7% with the nominal modulation wavelengths.

This result was also confirmed by TEM cross section studies. An example of TEM micrograph shown in Fig. 2 demonstrates a cross section of $[\mathrm{LSMO}\times 8\ \mathrm{u.c./YBCO}\times 3\ \mathrm{u.c.}]_{16}$ superlattice in which different layers can be clearly distinguished because of high atomic-number contrast between the layers. It is clear that the two oxides grow heteroepitaxially parallel to each other.

Figure 3(a) shows resistance versus temperature dependance of studied superlattices (Table I). This curve for $[\mathrm{LSMO}\times 16\ \mathrm{u.c./YBCO}\times 1\ \mathrm{u.c.}]_{16}$, LaY110, multilayer demonstrates a similar behavior as observed for single LSMO film.[12] An onset of the superconducting transition is seen starting from the sample LaY105 with 2 unit cells YBCO layer thickness. Beginning from the sample $[\mathrm{LSMO}\times 16\ \mathrm{u.c./YBCO}\times 3\ \mathrm{u.c.}]_{16}$, LaY107, a full transition to superconducting state is observed. One of the main reasons responsible for the suppression of superconducting state in the superlattice with 1 unit cells YBCO layers thickness and depression of superconducting transition tempera-

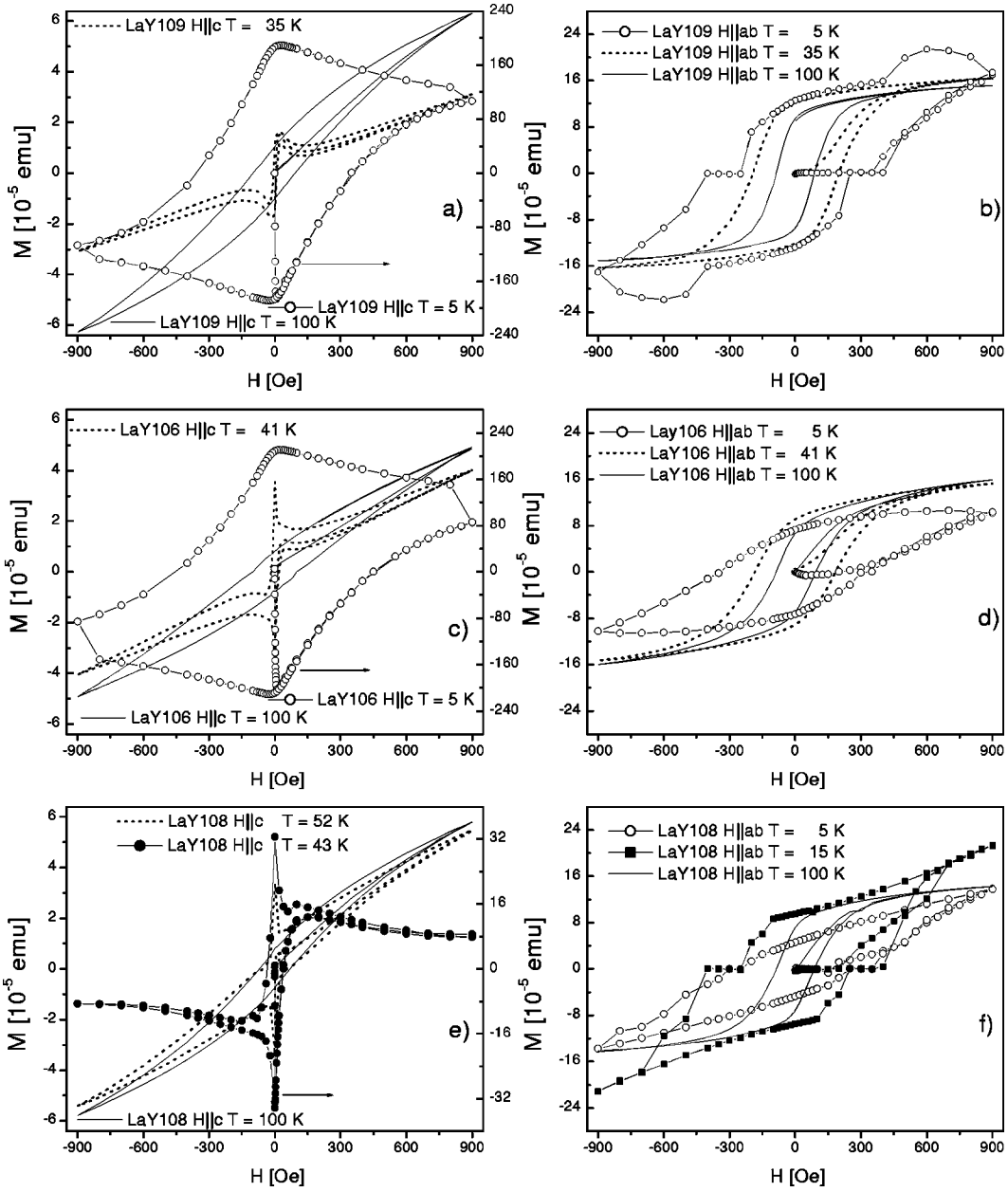

FIG. 6. Magnetization loops of the $[\mathrm{LSMO}\times 16$ u.c./$\mathrm{YBCO}\times n$ u.c.$]_{16}$ for $n=4,5,6$ unit cells YBCO layer thicknesses superlattices measured at 5 K to 100 K temperature range for magnetic field perpendicular ($H\|c$) and parallel ($H\|ab$) to the substrates.

ture in consecutive superlattices is a massive hole charge transfer from YBCO layers to LSMO layers. Recent elipsometric measurements[10] of far-infrared dielectric properties of LCMO/YBCO superlattices provide the evidence of a dramatic depletion of holes observed for about 1 nm thick YBCO layers which is due to the effect of hole charge transfer. For LSMO/YBCO multilayers an increase of hole concentration in LSMO layers can drive some of the layers into an antiferromagnetic state in spite of the $La_{0.67}Sr_{0.33}MnO_3$ nominal composition of LSMO films. For example in $YBa_2Cu_3O_7/PrBa_2Cu_3O_7$ (YBCO/PBCO) superlattices[17] even a sample with 1 unit cell YBCO layer thickness separated by 5 unit cells PBCO layer thickness is superconducting with T_{c0} higher than 50 K, indicating a limited hole transfer from YBCO layers to PBCO layers.

Figure 3(b) shows a zero-field cooling (ZFC) magnetic moment versus temperature of the measured multilayers (Table I). The superconducting transition temperature T_{d0} of the $[\mathrm{LSMO}\times 16$ u.c./$\mathrm{YBCO}\times n$ u.c.$]_{16}$ multilayers with $n=3$, 4, 5, 6, and 8 unit cells thicknesses are found to systematically increase with increasing YBCO layer thicknesses. Only for the $[\mathrm{LSMO}\times 16$ u.c./$\mathrm{YBCO}\times 3$ u.c.$]_{16}$, LaY107, superlattice a difference between T_{c0} and T_{d0} is observed. Such a difference was also observed for $[\mathrm{LSMO}\times 8$ u.c./$\mathrm{YBCO}\times n$ u.c.$]_{16}$ superlattices with $n=3$, 4 and 5 unit cells. The difference between the resistance transition temperature and the onset of the diamagnetic transition is a result of presence of the spontaneous vortex phase in this temperature interval as it was presented elsewhere.[13]

In Fig. 4 the ZFC and field cooling (FC) measurements of

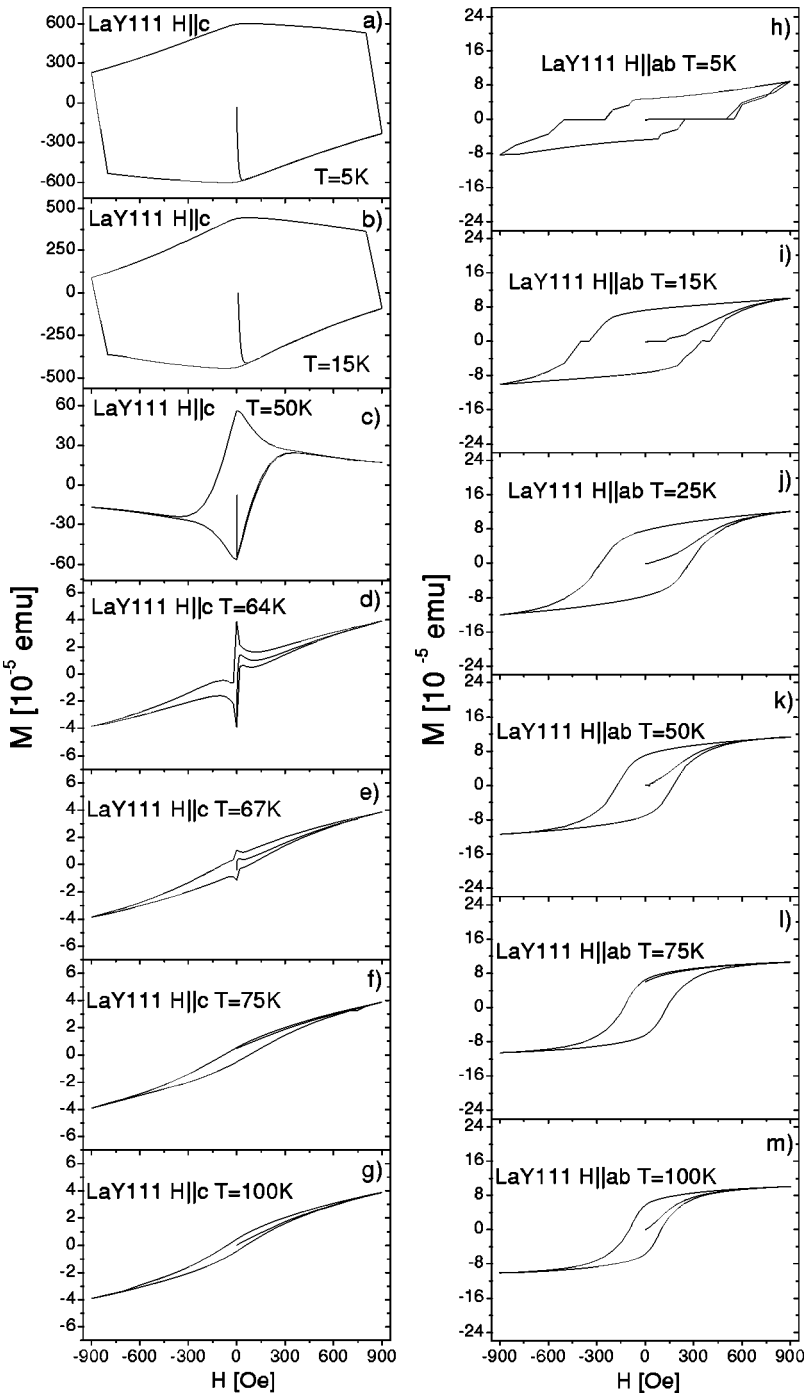

FIG. 7. Left panels: Magnetic hysteresis loops of $[\mathrm{LSMO}\times 16\ \mathrm{u.c./YBCO}\times 8\ \mathrm{u.c.}]_{16}$, LaY111, superlattice measured in the 5 K to 100 K temperature range for magnetic field perpendicular, $H\|c$, to the substrate. Right panels: Hysteresis loops measured in 5 K to 100 K temperature range for magnetic field parallel to the substrate, $H\|ab$.

the magnetic moment for samples LaY105, LaY109, LaY106, and LaY111 are shown. Both measurements were performed by warming up in 500 Oe after cooling in zero field and in 500 Oe, respectively. The ZFC and FC curves coincide at temperature higher than 120 K. The Curie temperature of a single LSMO layer is 360 K.[18,19] For studied multilayers the Curie temperature is higher than 300 K. The ZFC curves exhibit a broad peak in the temperature range from 50 K to 60 K, whereas the FC curves exhibit a steep change close to their superconducting transitions.

Magnetic hysteresis loops were measured in the 5 K to 100 K temperature range, with magnetic field along the two crystal orientations, i.e., parallel ($H\|ab$) and perpendicular ($H\|c$) to substrate as shown in Figs. 5, 6, and 7. It is evident that the magnetic moment always lies in the plane due to large shape anisotropy of measured multilayers. The in-plane [100] direction is the easy axis. For magnetic field perpendicular to the multilayers, i.e., [001] direction the hysteresis loops have a shape characteristic of the hard axes. This observation indicates that any interlayer exchange coupling in epitaxial $[\mathrm{LSMO}\times 16\ \mathrm{u.c./YBCO}\times n\ \mathrm{u.c.}]_{16}$ superlattices is related to the in-plane rotation of magnetic moments in consecutive LSMO layers, i.e., the ground state oscillates from antiparallel (AF) to parallel (F) moments of LSMO layers. In a recent paper[13] we reported the measurements of magnetic moment of $[\mathrm{LSMO}\times 8\ \mathrm{u.c./YBCO}\times n\ \mathrm{u.c.}]_{16}$ multilayers.

For such multilayers an easy axis of the magnetic moment switches from the in-plane to the out-of-plane configuration with an increase of thickness of YBCO spacer layers.

As shown in Figs. 5, 6, and 7 comparison of hysteresis loops recorded at temperature of 5 K and 100 K for magnetic field parallel to the samples ($H \| ab$) demonstrate an enhancement of coercivity at 5 K. This fact indicates that an unidirectional anisotropy is induced at the LSMO/YBCO interface.

It was observed[11] that when a ferromagnetic (F) film in contact with an AF thin film is cooled through the Neel point of the AF in applied magnetic field the hysteresis loop of the F develops a loop shift and enhances coercivity. The exchange biasing effects arises as the order of the AF is established in the presence of the F through the interfacial F-AF interaction. In the present case for the LSMO/YBCO superlattices due the hole charge transfer from YBCO layers into the LSMO layers 2 or 3 unit cells thick LSMO layers are converted into an AF state. Superlattices with 3 unit cells thick LSMO layers show zero net magnetic moment, similar as it was observed for LCMO/YBCO superlattices.[14]

The appearance of the response from superconducting YBCO layers in multilayered structure for magnetic field perpendicular to the sample ($H \| c$) is observed starting from the $[\mathrm{LSMO}\times 16\ \mathrm{u.c./YBCO}\times 3\ \mathrm{u.c.}]_{16}$, LaY107 superlattice [Fig. 5(e)]. For magnetic field $H \| c$ a response from YBCO layers is observed due to the large demagnetization factor for this configuration. For magnetic field H$\|$ab an appearance of superconducting phase is observed starting from the $[\mathrm{LSMO}\times 16\ \mathrm{u.c./YBCO}\times 4\ \mathrm{u.c.}]_{16}$, LaY109, multilayer [Fig. 6(b)]. The hysteresis loop recorded at $T=5$ K for $H \| ab$ exhibits superimposition of ferromagnetic moment from LSMO layers and the magnetic moment from superconducting YBCO layers. Similar behavior is also observed for $[\mathrm{LSMO}\times 16\ \mathrm{u.c./YBCO}\times n\ \mathrm{u.c.}]_{16}$ superlattices with $n=5$, 6, and 8 unit cells thick YBCO layers as shown in Fig. 5(d), 6(f), and 7(h). Furthermore, for these samples a plateau on *M-H* curves is observed, indicating an antiparallel alignment of the in-plane magnetic moments in consecutive LSMO layers. Antiparallel alignment of magnetic moments is a signature of interlayer exchange coupling between LSMO layers through superconducting YBCO layers, similar as it was observed for the metallic tunnel junctions[15,16] confirmed by magnetoresistance measurements.

Illustration of the evolution of hysteresis loops in the 5 K to 100 K temperature interval for both configurations of magnetic field of $[\mathrm{LSMO}\times 16\ \mathrm{u.c./YBCO}\times 8\ \mathrm{u.c.}]_{16}$, LaY111 superlattice is shown in Fig. 7. The hysteresis loops for magnetic field perpendicular to the sample are presented in the left panel of Fig. 7. The *M-H* curves evolve from typical superconducting loops below superconducting critical temperature $T_{c0}=71$ K to typical ferromagnetic above this temperature.

Close to the superconducting transition temperature [Figs. 7(d) and 7(e)] the hysteresis loops show a complex behavior that is due to the interplay between Meissner currents in YBCO layers and the magnetic fields present in LSMO layers. For magnetic field parallel to the sample due to diminished role of the demagnetization factor only at $T=5$ K a response from YBCO layers is observed.

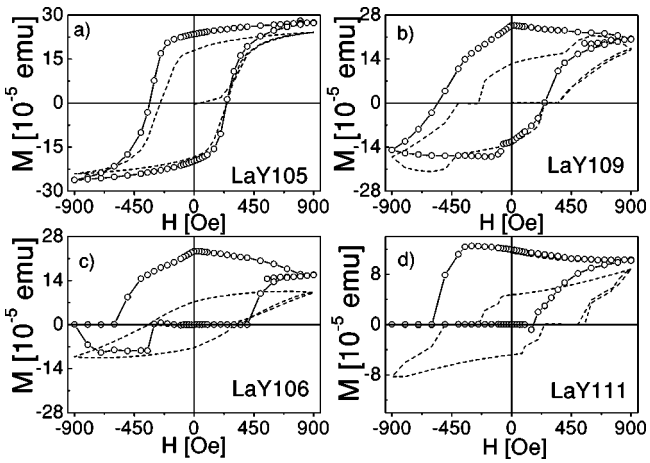

FIG. 8. Hysteresis loops recorded at temperature 5 K after ZFC from above 300 K (dotted line) and FC (solid line) in field of 500 Oe ($H \| ab$) of LSMO/YBCO superlattices with 2, 4, 5, and 8 unit cells YBCO layer thickness.

As already mentioned at LSMO/YBCO interfaces a hole charge transfer from YBCO layers to LSMO layers takes place. According to the phase diagram[20] of the $La_{1-x}Sr_xMnO_3$ system for the doping level $x>0.48$ an antiferromagnetic phase is observed. Therefore in LSMO/YBCO multilayers a part of LSMO layers (2 or 3 unit cells) are driven into an antiferromagnetic state due to this effect. When an F/AF interfaces are cooled through the Neel temperature T_N with $T_C > T_N$ an unidirectional anisotropy is induced in F layers.

In Fig. 8 magnetic hysteresis loops measured at temperature 5 K after ZFC and FC in 500 Oe for $[\mathrm{LSMO}\times 16\ \mathrm{u.c./YBCO}\times n\ \mathrm{u.c.}]_{16}$ superlattices with $n=2$, 4, 5, and 8 unit cells of YBCO layer thickness are shown. It is evident that ZFC loops are symmetric around zero field, while the FC loops are shifted towards negative fields. This effect is a result of induced unidirectional anisotropy at LSMO layers.

According to the model of Sa de Melo[1] an interlayer exchange coupling is possible between the LSMO layers across YBCO layers with the period of $Lz=2.4$ nm. The model suggests an optimal Fermi wave vector along [001] direction $k_F=\pi/2c$, which means that $k_F d_S=10$, hence a $d_S=7{,}64$ nm, i.e., approximately 6 to 7 *c* axis unit cells. This effect should be observable for superconducting spacer thickness less than 13 nm. The observed exchange biasing effects for LSMO/YBCO multilayers additionally support the presence of hole charge transfer effect. The result of the shift of the hysteresis loops along field axis, the sign and the magnitude of the shift is a quantitative measure of the interlayer coupling.

The exchange biasing in manganite type heterostructures was observed in $La_{2/3}Ca_{1/3}MnO_3/La_{1/3}Ca_{2/3}MnO_3$ multilayers,[21] $La_{2/3}Ba_{1/3}MnO_3/LaNiO_3La_{2/3}Ba_{1/3}MnO_3/La_{1/3}Ca_{2/3}MnO_3$ four-layers heterostructures,[22] $La_{0.67}Ca_{0.33}MnO_3/La_{0.5}Ca_{0.5}MnO_3$ bilayers,[23] and $La_{0.7}Sr_{0.3}MnO_3/La_{0.33}Ca_{0.67}MnO_3$ bilayers.[24]

For the LaY105 superlattice, i.e., with 2 unit cells YBCO

layer thickness [Fig. 8(a)] the obtained exchange biasing field is $H_{EB}=41$ Oe. Thus the estimated unidirectional interface energy $\Delta J=M_S H_{EB}\, d_F$, for this sample, where M_S is the saturation magnetization and d_F is the thickness of LSMO layer, 4×10^{-3} erg/cm^2, and is lower than energies reported for other multilayers.[21] The obtained exchange biasing field for samples LaY106, LaY109, and LaY111 is 94 Oe, 149 Oe, and 218 Oe respectively.

Hysteresis loops recorded in FC mode for superlattices with 4, 5, and 8 unit cells YBCO layer thicknesses in addition demonstrate a shift along vertical (M) axis as shown in Figs. 8(b)–8(d). The shift along M axis could be a result of the interaction between the shielding currents induced in YBCO layers during FC process and magnetic field in LSMO layers. An observation of exchange biasing effect in LSMO/YBCO superlattices indicates the presence of interlayer exchange coupling between LSMO layers through the superconducting YBCO spacer layers.

IV. CONCLUSIONS

In summary, we have grown high-quality LSMO/YBCO superlattices. XRD and TEM studies indicate that superlattices have a well defined superlattice structure. An onset of superconductivity is observed starting from the sample with 2 unit cells of YBCO layers thickness in multilayered structure. The exchange -biasing mechanism sets in LSMO/YBCO superlattices. Unidirectional anisotropy in LSMO layers is observed due to hole charge transfer from YBCO layers to LSMO layers. The demonstration of exchange biasing effect in LSMO/YBCO superlattices indicates an existence of interlayer exchange coupling between LSMO layers through YBCO superconducting spacer layers.

ACKNOWLEDGMENTS

This work was supported by Committee for Scientific Research (KBN) under Grant Nos. 5P03B 06220 and 2 P03B 05 024.

[1] C.A.R. Sa de Melo, Physica C **387**, 17 (2003).
[2] C.A.R. Sa de Melo, Phys. Rev. Lett. **79**, 1933 (1997); Phys. Rev. B **62**, 12 303 (2000).
[3] S.A. Wolf, D.D. Awschalom, R.A. Buhrman, J.M. Daughton, S. von Molanar, M.L. Roukes, A.Y. Chtchelkanova, and D.M. Treger, Science **294**, 1488 (2001).
[4] J.H. Park *et al.*, Nature (London) **392**, 794 (1998).
[5] G. Jakob, V.M. Moschalkov, and Y. Bruynseraede, Appl. Phys. Lett. **66**, 2564 (1995).
[6] P. Przyslupski, S. Kolesnik, E. Dynowska, T. Skoskiewicz, and M. Sawicki, IEEE Trans. Appl. Supercond. **7**, 2192 (1997).
[7] A.M. Goldman, V. Vasko, P. Kraus, K. Nikolaev, and V.A. Larkin, J. Magn. Magn. Mater. **200**, 69 (1999).
[8] H.U. Habermeier, G. Cristiani, R.K. Kremer, O. Lebedev, and G.V. van Tendeloo, Physica C **364-365**, 298 (2001).
[9] P. Prieto, V. Vivas, G. Campillo, E. Baca, L.F. Castro, M. Varela, C. Ballestros, J. Villegas, D. Arias, C. Leon, and J. Santamaria, J. Appl. Phys. **89**, 8026 (2001).
[10] Todd Holden, H.U. Habermeier, G. Cristiani, A. Golnik, A. Boris, A. Pimenow, J. Humellcek, O. Lebedev, G. Van Tendello, B. Keimer, and C. Bernhard, Phys. Rev. B **69**, 064505 (2004).
[11] J. Nouges and Ivan K. Schuler, J. Magn. Magn. Mater. **192**, 203 (1999).
[12] P. Przyslupski, T. Nishizaki, N. Kobayashi, S. Kolesnik, T. Skoskiewicz, and E. Dynowska, Physica B **259-261**, 820 (1999).
[13] P. Przyslupski, I. Komissarov, W. Paszkowicz, P. Dluzewski, M. Sawicki, and R. Minikayev, J. Appl. Phys. **95**, 2906 (2004).
[14] Z. Sefrioui, D. Arias, V. Pena, J.E. Villegas, M. Varela, P. Prieto, C. Leon, J.L. Martinez, and J. Santamaria, Phys. Rev. B **67**, 214511 (2003).
[15] T. Miyazaki and N. Tezuka, J. Magn. Magn. Mater. **139**, L231 (1995).
[16] M. Tanaka, Y. Higo, and S. Sugahara, J. Supercond. **16**, 241 (2003).
[17] G. Jakob, P. Przyslupski, C. Stolzel, C. Tome-Rosa, A. Walkenhorst, M. Schmidt, and H. Adrian, Appl. Phys. Lett. **59**, 1626 (1991).
[18] J.H. Park, E. Vescono, H.J. Kim, C. Kwon, R. Ramesh, and T. Venkatesan, Phys. Rev. Lett. **81**, 1953 (1998).
[19] M. Zeise, H.C. Semmelhack, and P. Busch, J. Magn. Magn. Mater. **246**, 327 (2002).
[20] Y. Tokura and Y. Tomioka, J. Magn. Magn. Mater. **200**, 1 (1999).
[21] I. Panagiotopoulos, C. Christides, D. Niarchos, and M. Pissas, Phys. Rev. B **60**, 485 (1999); J. Appl. Phys. **87**, 3926 (2000).
[22] K.R. Nikolaev, A.Yu. Dobin, I.N. Krivorotov, W.K. Coley, A. Bhattacharya, A.L. Kobrinskii, L.I. Glazman, R.M. Wentzovitch, E. Dan Dahlberg, and A.M. Goldman, Phys. Rev. Lett. **85**, 3728 (2000).
[23] H.B. Peng, X.X. Zhang, Z. Xie, H.J. Tao, B. Xu, H. Liu, and B.R. Zhao, Phys. Rev. B **61**, 8955 (2000).
[24] D.-W. Kim, T.W. Noh, H. Tanaka, and T. Kawai, Solid State Commun. **125**, 305 (2003).